Rapid diversification and dispersal during periods of global warming by plethodontid salamanders

David R. Vieites[†‡], Mi-Sook Min[§], and David B. Wake[†‡]

[†]Museum of Vertebrate Zoology and Department of Integrative Biology, University of California, Berkeley, CA 94720-3160; and [§]BK21 Program for Veterinary Science and Conservation Genome Resource Bank for Korean Wildlife, Seoul National University, Seoul 151-742, South Korea

Edited by Michael J. Donoghue, Yale University, New Haven, CT, and approved October 22, 2007 (received for review May 29, 2007)

A phylogeny and timescale derived from analyses of multilocus nuclear DNA sequences for Holarctic genera of plethodontid salamanders reveal them to be an old radiation whose common ancestor diverged from sister taxa in the late Jurassic and underwent rapid diversification during the late Cretaceous. A North American origin of plethodontids was followed by a continental-wide diversification, not necessarily centered only in the Appalachian region. The colonization of Eurasia by plethodontids most likely occurred once, by dispersal during the late Cretaceous. Subsequent diversification in Asia led to the origin of *Hydromantes* and *Karsenia*, with the former then dispersing both to Europe and back to North America. Salamanders underwent rapid episodes of diversification and dispersal that coincided with major global warming events during the late Cretaceous and again during the Paleocene–Eocene thermal optimum. The major clades of plethodontids were established during these episodes, contemporaneously with similar phenomena in angiosperms, arthropods, birds, and mammals. Periods of global warming may have promoted diversification and both inter- and transcontinental dispersal in northern hemisphere salamanders by making available terrain that shortened dispersal routes and offered new opportunities for adaptive and vicariant evolution.

historical biogeography | paleogeography | Plethodontidae
dispersal | salamander phylogeny | phylogeny

Plethodontidae, the most speciose family of salamanders, is also the most differentiated in morphology, ecology, and behavior. The family includes ≈68% of the extant described species of caudate amphibians (1). New analyses of mtDNA, nuclear DNA, and morphology (2–6) have achieved consensus on many aspects of phylogenetic relationships, but unresolved conflicts remain. The disjunct and highly asymmetric Holarctic distribution of the family, with ≈98% of the species in the Americas and a few in the Mediterranean region, has long been a biogeographic puzzle (7–9), with the debate centered on the timing and route of colonization of Eurasia (reinvigorated with the recent discovery of *Karsenia*, the first East Asian plethodontid; ref. 10). The distribution of the supergenus (Sg) *Hydromantes*, with representatives in western North America and in the Mediterranean, has been considered enigmatic, even paradoxical, given the high degree of philopatry, small ranges, and low dispersal capacity of plethodontids (11). Two hypotheses have been proposed: a dispersal event from eastern North America to Europe across the Paleocene–Eocene North Atlantic land bridge (NALB) (12, 13), or via later Cenozoic movement across the Bering land bridge, from western North America to Europe (8). Plethodontidae are thought to have originated in the Appalachian region, because of ideas of the origin of lunglessness (universal in the family), the presence of many early branched lineages in the region, and the great age of the mountain system (14, 15), but these ideas have been questioned (2, 16). New phylogenetic analyses identify long-established lineages in western North America, and some clades are spread across the continent. Here we test hypotheses on the origin, dispersal, and pattern of diversification of the main lineages in the family by generating a large nuclear sequence dataset (≈2.7 kb per species from 3 single-copy protein-coding nuclear genes for 43 salamander taxa, and several outgroups), which we analyze to produce a robust phylogenetic hypothesis, as well as hypotheses on the origin and times of divergence of the main lineages. Our focus is the evolutionary history, phylogenetic relationships, and historic biogeography of Holarctic plethodontids. Although some bolitoglossines, which account for 60% of plethodontids, are included here, this deeply nested clade centered in the American tropics is treated elsewhere (17).

Results and Discussion

Phylogenetic Relationships Among Plethodontids. Our results require taxonomic changes, explained in supporting information (SI) *Text*. Two major clades are recovered with strong statistical support (Fig. 1); the Plethodontinae (including *Plethodon*, *Karsenia*, Sg *Hydromantes*, *Ensatina*, Sg *Desmognathus*, and *Aneides*) and the Hemidactyliinae. Two subclades of Hemidactyliinae are recovered, one of which (Spelerpini: *Eurycea*, *Gyrinophilus*, *Pseudotriton*, *Stereochilus*) is well supported, and the other (including *Hemidactylium*, *Batrachoseps*, and Sg *Bolitoglossa*) with less statistical support. Shimodaira-Hasegawa nonparametric likelihood ratio test (SHT) results, congruent with the maximum likelihood (ML) support values, were unable to reject different placements on the tree (SI Table 1), but the strong Bayesian support for the exclusively North American lineages (*Plethodon* and relatives) leaves *Karsenia* and Sg *Hydromantes*, recovered as sister taxa, outside that clade. Sg *Hydromantes* is monophyletic, with two major clades corresponding to European and North American species. A monophyletic *Plethodon* is sister to a clade of the remaining taxa, for which support is not strong. *Ensatina* is sister to Sg *Desmognathus* (itself a well supported clade) + *Aneides*. *Aneides* is monophyletic, with the eastern species (*A. aeneus*) sister to a clade constituted of the central (*A. hardii*) + western species. *Plethodon* contains two well supported subclades corresponding to the eastern and western species. Eastern small and eastern large species of *Plethodon* also constitute two reciprocally monophyletic clades. Data are significantly less supportive of paraphyly of *Plethodon*, with *Aneides* nested within it (SHT; SI Table 1).

Timescale for Plethodontid Origin and Diversification. Major issues in dating cladogenetic events by using fossil and biogeographic data and molecularly based phylogenetic hypotheses are the frequent

Author contributions: D.R.V. and D.B.W. designed research; D.R.V. performed research; D.R.V. analyzed data; and D.R.V., M.-S.M., and D.B.W. wrote the paper.

The authors declare no conflict of interest.

This article is a PNAS Direct Submission.

Data deposition: The sequences reported in this paper have been deposited in the GenBank database (accession nos. EU275780–EU275901).

[‡]To whom correspondence may be addressed. E-mail: vieites@berkeley.edu and wakelab@berkeley.edu.

This article contains supporting information online at www.pnas.org/cgi/content/full/0705056104/DC1.

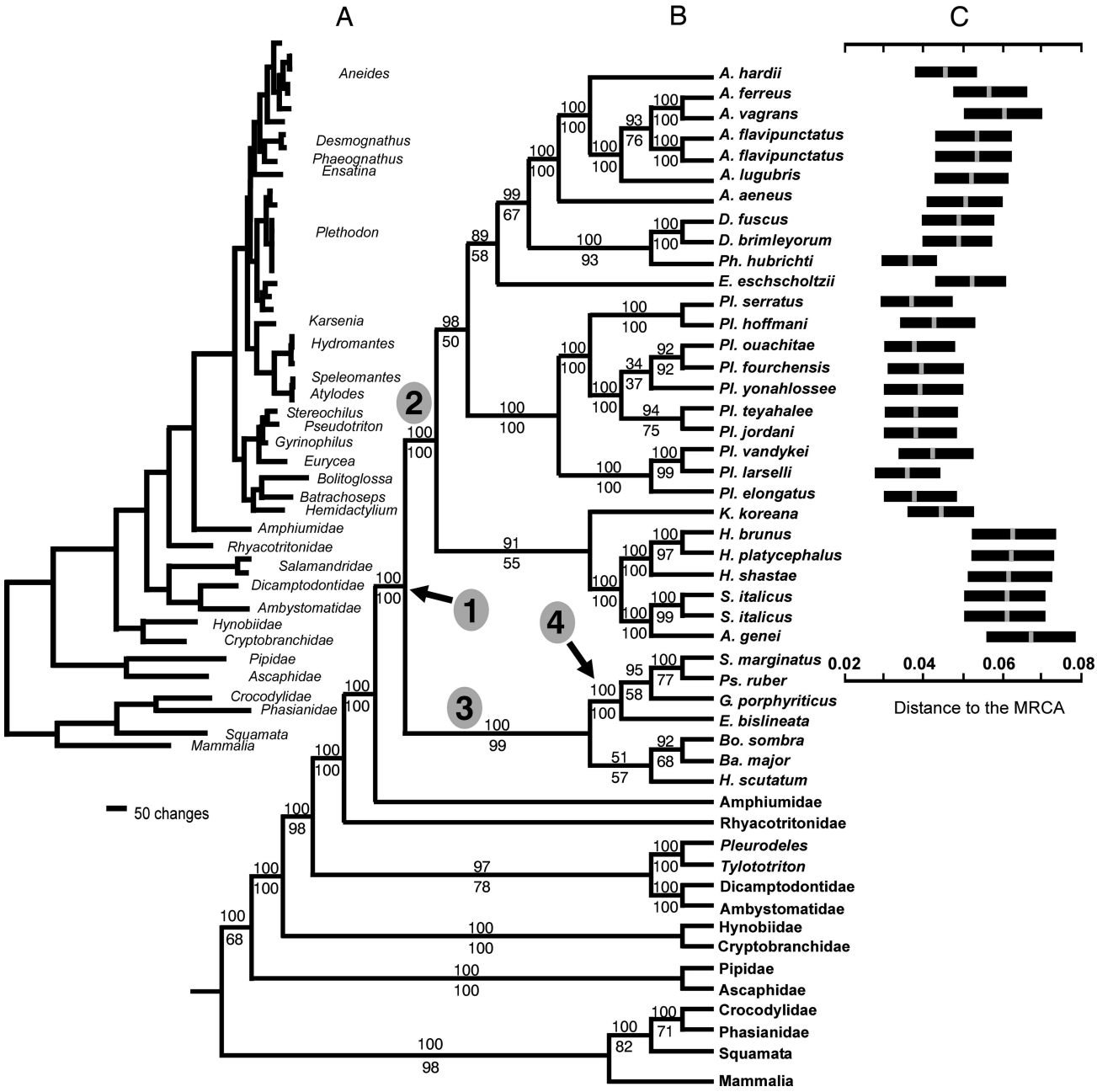

Fig. 1. Phylogenetic relationships of Holarctic plethodontids. (*A*) ML phylogram. (*B*) The 50% majority consensus rule cladogram of trees resulting from Bayesian analyses. Upper values on nodes represent Bayesian posterior probability, and lower ones represent ML bootstrap proportion. (*C*) Bayesian relative rate tests showing the relative branch length for every species using spelerpines as most recent common ancestor; note that most rapid rates of evolution occurred in Sg *Hydromantes*. In the cladogram, numbers encircled in gray refer to family Plethodontidae (1), subfamilies Plethodontinae (2) and Hemidactylinae (3), and tribe Spelerpini (4), respectively.

differences in evolutionary rates among genes and taxa (18) as well as the accuracy of the age constraints available (19). We used a partitioning scheme and relaxed molecular clock method (20). We investigated the effects of constraining some nodes with well supported dating based on paleontological criteria (21). Preliminary tests suggested that these parameters often have strong effects on time estimates, especially on 95% confidence intervals (*SI Text*). Multiple age constraints give more accurate estimates for young nodes, but inclusion of ancient, well constrained nodes (21) is critical to estimate old splits. Although this suggests that but a few such calibrations would be sufficient to estimate ancient splits, younger constraints are necessary to adequately estimate divergences for recent splits.

Our analyses (Fig. 2 and SI Table 2) agree with other studies in dating the split between frogs and salamanders in the Carboniferous (19, 22–25). This age and that recently estimated for the split between amphibians and amniotes (late Devonian; ref. 26) seem too old according to the fossil record (27). A Mesozoic origin for salamanders has been proposed based on the fossil record (28, 29), and by most of the molecular studies available so far (19, 24, 25), although a late Paleozoic diversification of salamanders has also been suggested (23). Our data are in agreement with other studies (19, 25) that date the initial split within modern salamanders almost immediately after the Permo-Triassic mass extinction. A younger origin, in the Juras-

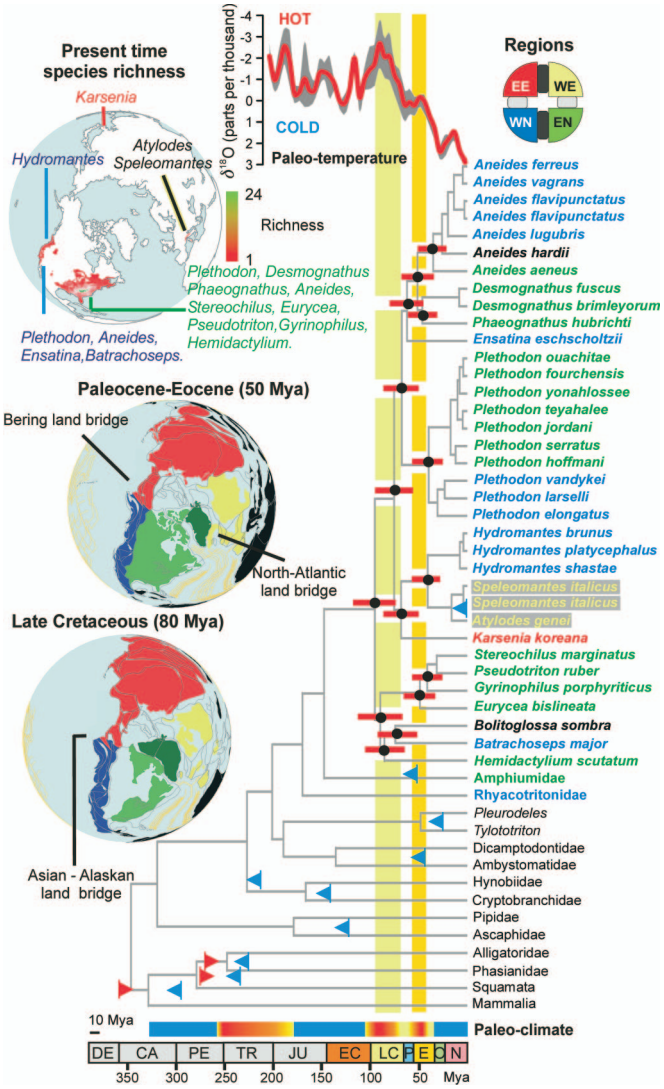

Fig. 2. Chronogram for the taxa analyzed. Data were calculated with MULTIDIVTIME using a prior of 20 mya for *rttmsd*, a *bigtime* of 420 mya, and lower fossil constraints. Branch lengths are proportional to time units. Red bars represent 95% confidence intervals; blue and red triangles represent minimum and maximum fossil time constraints, respectively. At the top right, a color-coded wheel represents the four main regions considered: EE (red), eastern Eurasia; WE (yellow), western Eurasia; EN (green), eastern North America; WN (blue), western North America. The same color-coding scheme was applied to species names and paleogeographic reconstructions for the Paleocene–Eocene and Late Cretaceous (shown at left). Tectonic plates and ocean isochrones are overlapped in gray and orange, respectively (29). Actual species richness for the Holarctic plethodontid genera is represented at top left. All geographic reconstructions are orthographically projected, with −60° set as the central meridian and 85° set as the reference latitude. At the top of the chronogram is a chart representing the evolution of the deep-sea oxygen δ^{18} isotope across time, with the smoothed mean highlighted in red and the 75% interval in gray. Paleoclimate is indicated by a bar at the bottom coded from blue to red, representing glaciations and cold-to-hot periods, respectively. Time scale is shown at the bottom, with letters representing geologic periods (DE, Devonian; CA, Carboniferous; PE, Permian; TR, Triassic; JU, Jurassic; EC, Early Cretaceous; LC, Late Cretaceous; P, Paleocene; E, Eocene; O, Oligocene; N, Neogene).

sic, has been proposed (24); although that study used methods similar to ours, only a single fossil age constraint was used, as well as a combination of parameter values (old *bigtime* value, *rttmsd* constrained to 10 million years) that we show (*SI Text*) consistently underestimate divergence times.

The warm temperate climate in proto-Laurasia during the early Jurassic (Fig. 2; ref. 30) favored the diversification of many salamander lineages, which, according to our estimates, diverged in a relatively short period, predating the split of Pangea. Amphiumids and the ancestor of plethodontids diverged in the mid-Jurassic, but the initial split within plethodontids did not occur until the Late Cretaceous, just after the early Cretaceous glaciation (Fig. 2). Paleoclimatic reconstructions (Fig. 2) show two global warming periods: late Cretaceous and at the Paleocene–Eocene boundary. These periods coincide with episodes of rapid lineage diversification of plethodontids, as evidenced by the short internodes shown in the ML phylogram (Fig. 1). Low extinction rates might account for short internodes, but we would not expect to see the pattern of clustering at particular time intervals that we find.

Historical Biogeography of Plethodontids. Plethodontids long were thought to have originated from stream-dwelling forms living in Appalachia that had lost lungs as a rheotropic adaptation (31). Appalachia was indicated by the high number of extant species and adaptive diversity in an old and stable mountain system (Fig. 2). A large molecular dataset was interpreted as either challenging (2) or supporting (3) this idea. The origin of lunglessness also has been debated (16, 31–34), and an analysis in the context of geologic history favored an Appalachian origin but did not reject a western North American or eastern Asian origin (16). We combined a robust phylogenetic hypothesis for all Holarctic genera, divergence time estimates, paleographic reconstructions, and a biodiversity analysis to examine the "Out of Appalachia" hypothesis. We propose an alternative scenario that agrees with all data available.

The major clades, Plethodontinae and Hemidactyliinae, both have representatives in eastern and western North America. The split between them is dated in the mid-Cretaceous ≈94 mya (SI Table 2). During the early Cretaceous, eastern and western North America were physically connected, but from ≈110 to 70 mya, increasing sea levels generated a marine midcontinental seaway separating these regions (Fig. 2; ref. 35). The Appalachian Mountains originated in the late Precambrian. By the end of the Mesozoic, they were mostly eroded, uplifting again during the Cenozoic. By the time the two main clades split, other mountain systems existed on the continent. A major vicariant event associated with the epicontinental seaway is the most parsimonious scenario for the early diversification of plethodontids, but our divergence time estimates suggest more recent transcontinental movements for *Aneides* and *Plethodon* (Fig. 2 and SI Table 2). *Plethodon* and *Aneides* occur in both eastern and western North America, with a large midcontinental gap and isolated species in New Mexico. Other taxa with low dispersal capacities (e.g., spiders; ref. 36) display a similar pattern. During the Paleocene–Eocene thermal maximum (PETM) and Eocene thermal optimum (Fig. 2), diversification was higher, with splits of *Aneides* from the ancestor of *Desmognathus* and *Phaeognathus*, *Eurycea* from *Gyrinophilus*, *Desmognathus* from *Phaeognathus*, and *Hydromantes* from *Speleomantes* and *Atylodes*. Current diversity estimates (Fig. 2 *Top*) can be misleading if the ages of the clades are not considered. *Plethodon* and *Desmognathus* are the most speciose genera among the Plethodontinae, with centers of diversity in the Appalachian Mountains. However, these are relatively recent and rapid radiations, with high lineage accumulation in recent geologic times (6, 37), probably favored by the uplift of Appalachia in the Cenozoic and the reacquisition of aquatic larvae by desmognathines (2). The high species diversity in Appalachia corresponds mainly to recent radiations, but the ancestor of the family could have been distributed anywhere in North America. This hypothesis is supported by ancestral range reconstructions using Lagrange(ref. 38; *SI Text*). The biogeographic scenario with highest likelihood (L) suggests a widespread distribution for the common ancestor of the family in

eastern and western North America, an eastern North American origin having lower statistical support. Of the four hemidactyline clades, only Spelerpini fits the original model of Appalachian origin.

Colonization of Eurasia by Plethodontids and Holarctic History. Northern hemisphere biogeography has been characterized by major dispersal events between Eurasia and North America, but the routes and timing of such events are debated (39, 40). Allozymic studies favored a divergence time of ≈50 mya between North American and European members of Sg *Hydromantes*, the NALB being suggested as the dispersal route (9, 13). The recent discovery of *Karsenia koreana* (10) in northeastern Asia raised new hypotheses including two independent origins: dispersal via Beringia to account for *Karsenia*, and via the NALB to account for *Speleomantes* + *Atylodes* (41). Our data and analyses suggest a different scenario. During the late Cretaceous, diversification of plethodontid lineages occurred rapidly, culminating in ancestors, or the common ancestor, of *Karsenia* and Sg *Hydromantes*, which probably diverged from other lineages in western North America. Ancestral range reconstruction (38) gives highest support to this scenario (L = −238.98), but a western North American–eastern Eurasian ancestral range is also statistically significant (L = −239.74). During the late Cretaceous, warm temperate conditions in the northern hemisphere would have facilitated colonization of new habitats and dispersal to far northern latitudes. These environmental changes coupled with geological connections between Eurasia and North America would have shortened transcontinental migration routes. The epicontinental seaway separated eastern and western North America, and the Turgai Sea separated eastern from western Eurasia, making the land bridge that connected western North America and eastern Eurasia (Fig. 2) the most parsimonious scenario for dispersal to Eurasia. We hypothesize a single colonization event followed by rapid diversification in the Holarctic, the split between *Karsenia* and Sg *Hydromantes* lineages taking place in Asia just after the K/T boundary (≈65 mya). During the PETM, Eurasia was connected to North America through the Bering land bridge and the NALB (Fig. 2), although by ≈55 mya, the land connection was submerged (42). Our estimate of divergence time between North American *Hydromantes* and European *Speleomantes* + *Atylodes* is ≈41 mya (SI Table 2). The most parsimonious biogeographic scenario from perspectives of paleogeography, divergence time estimates, and the biology of the species (i.e., low dispersal capacity and high degree of philopatry; ref. 11) is that *Hydromantes* dispersed from northeast Asia both back to western North America and to western Eurasia. Ancestral range reconstruction analyses suggest that the ancestor of Sg *Hydromantes* was distributed both in western North America and eastern Eurasia (L = −238.76). A distribution only in eastern Eurasia is also statistically significant (L = −240.44). Given the likelihood that the common ancestor of Sg *Hydromantes* was distributed both in western North America and eastern Eurasia, a final alternative to consider is the origin of Sg *Hydromantes* in western North America; the ancestor of the European clade might have crossed the Bering land bridge to Asia and western Europe at a later date than the ancestor of *Karsenia*. This hypothesis is unlikely considering the biological features mentioned above, because it would have required much more dispersal (double the distance of the most likely scenario).

Episodes of Global Change Correspond with Rapid Lineage Diversification. The diversification of plethodontid lineages occurred during short time spans, no matter what time estimation method is used, as reflected by the short internodes recovered (Fig. 1). Two major episodes of lineage diversification are detected, one in the late Cretaceous and one during the PETM continuing into the Eocene thermal optimum. A similar pattern has been recognized in both birds and mammals (43, 44), with a radiation of major clades in the late Cretaceous followed by a slowing of diversification rate until the PETM, although this was recently challenged for mammals (45) and debate on this issue is still open. Other taxa, including ants and angiosperms, underwent similar diversification episodes (46). The concordance of these events well before and after the end-of-Cretaceous extinctions suggests that they could have been driven by similar factors. Late Cretaceous and PETM experienced global warming events, with significantly higher temperatures in northern latitudes (30, 47). Although global warming may have driven many taxa to extinction, it also may have been a major factor stimulating the diversification of others, generating some uncertainty about what will happen to modern biodiversity under future global warming scenarios. The diversification of angiosperms during Cretaceous warming would have provided new ecological niches suitable for several groups, both vertebrates and invertebrates (26, 44, 46), stimulating their diversification. The spectacular diversification and dispersal of modern groups of mammals and birds also has been linked to rapid global warming during the same periods (48, 49). Global warming periods could have been particularly favorable for dispersal of even the unlikely dispersing salamanders, as well as other tetrapods, and clades of invertebrates and plants, but the causes (i.e., climatic, ecological because of the availability of new resources and niches, or physical by shortening distances) are unknown. Plethodontid salamanders today have a restricted distribution in Eurasia, but they must have been more widespread in the past, leaving open the possibility of new discoveries.

Materials and Methods

Taxon and Gene Sampling. We sampled all Holarctic plethodontid genera, including *Batrachoseps*, which is primarily Californian in distribution. *Bolitoglossa*, representing the neotropical lineage, seven additional salamanders, and six other tetrapods provide a backbone phylogeny and age constraints for divergence dating analyses. *Protopterus sp.* was used as a general outgroup. Voucher and sequence information are included in SI Table 3. By using standard PCR and sequencing techniques, we obtained sequence data from three nuclear protein-coding genes: 1,459 aligned bp from recombination activating gene 1 (RAG1), 713 aligned bp from brain-derived neurotrophic factor (BDNF), and 535 aligned bp from proopiomelanocortin (POMC). These markers were selected because (*i*) they are protein-coding single-copy genes, located in different regions of the nuclear genome, (*ii*) they vary in degree of conservation, being suitable for deep and shallow phylogenetic inference, and (*iii*) they are suitable for reconstruction of ancient relationships (50) and for time estimations (51). For primers (52) and sequence parameters see SI Table 4.

Phylogenetic Inference. We inferred phylogenies using ML and Bayesian inference methods. One thousand nonparametric bootstrap ML repetitions were conducted by using Garli v0.94 (53) under the GTR model, and analyses were repeated three times to test for congruence. We performed analyses using different partition strategies, applying the Akaike Information Criterion to determine the evolutionary models and parameters that best fit each partition (SI Table 4). We performed two independent Bayesian analyses, using a ML starting tree and running four Markov chains sampled every 1,000 generations for 40 million generations with Mr Bayes v3.1 (54). Remaining trees after burnin of 20 million generations were combined, and the 50% majority consensus tree was calculated by using PAUP* 4b10 (55). Alternative placements of some genera were tested with SHT (56). Details on implementing phylogenetic methods are included as (*SI Text*).

Divergence Dating. We used Bayesian relative rate tests (57) to test for constancy of evolutionary rates among plethodontids, and to test whether the differences are associated with any major clado-

genetic or biogeographic events. To estimate divergence times among clades, we used a relaxed molecular clock Bayesian approach implemented in the package MULTIDIVTIME (20). The potential effects of priors, fossil constraints, and our partitioning strategy were tested by performing multiple analyses with different combinations of parameters. Because the salamander fossil record is uneven, we included several well constrained splits outside amphibians for our divergence time estimation, and used seven calibration events based on amphibian fossils. Because constraining nodes based on the tetrapod fossil record has generated controversy (21, 58), we performed analyses with and without those constraints. Comprehensive information on the divergence dating analyses, fossils, and age constraints used is found in *SI Text*.

Diversity Estimates and Paleoreconstructions. Distribution maps (59) were projected to an equal area grid of 0.25 arcmin per cell in ArcInfo, and the species richness (number of species per grid cell) was calculated for all plethodontid genera in the Holarctic. Paleoreconstructions were made of Earth in the Late Cretaceous and the Paleocene/Eocene (Fig. 2; ref. 35), the latter slightly modified to incorporate the NALB (60). In both, sea levels during these periods were estimated (35, 60). Paleotemperature reconstruction is based on a compilation of oxygen isotope measurements of benthic foraminifera, which reflect local temperature changes in their environment (30, 61); paleoclimate (Fig. 2) follows Frakes *et al.* (62). The mean and 75% confidence intervals were calculated for each 5-million-year period and smoothed in a 2-million-year sliding window. The evolution of geographic ranges using a phylogenetic hypothesis, divergence times, dispersal and extinction rates, and a paleogeographic scenario were modeled in a likelihood framework by using Lagrange 1.0 (38). The method provides likelihood values for the different biogeographic scenarios, enabling reconstruction of ancestral ranges and inference of directionality of dispersal events. A range of extinction and dispersal parameters were explored; see *SI Text*.

We thank S. Nieto Román, H. B. Shaffer, M. H. Wake, R. Bonett, J. Wiens, P. Chippindale, W. Clemens, J. Patton, two anonymous reviewers, and the D.B.W. laboratory group for discussion and comments, as well as T. Papenfuss for computer support. J. Thorne provided valuable help with Multidivitime, and R. A. Duncan, R. C. Blakey, and C. Scotese helped with Holarctic paleogeography. Tissues were provided by the Museum of Vertebrate Zoology, Louisiana Museum of Natural History, and G. Nascetti for European species. Laboratory work and fieldwork were supported by National Science Foundation Grant EF-0334939.

1. AmphibiaWeb: Information on Amphibian Biology and Conservation. Available at http://amphibiaweb.org/. Accessed April 10, 2007.
2. Mueller RL, Macey JR, Jaekel M, Wake DB, Boore JL (2004) *Proc Natl Acad Sci USA* 101:13820–13825.
3. Macey JR (2005) *Cladistics* 21:194–202.
4. Chippindale PT, Bonett RM, Baldwin AS, Wiens JJ (2004) *Evolution* 58:2809–2822.
5. Wiens JJ, Bonett RM, Chippindale PT (2005) *Syst Biol* 54:91–110.
6. Wiens JJ, Engstrom TN, Chippindale PT (2007) *Evolution* 60:2585–2603.
7. Darlington PJ (1957) *Zoogeography: The Geographical Distribution of Animals* (Wiley, New York).
8. Wake DB, Maxson LR, Wurst GZ (1978) *Evolution* 32:529–539.
9. Lanza B, Caputo V, Nascetti G, Bullini L (1995) *Mus Reg Sci Nat Monog (Torino)* 16:1–366.
10. Min MS, Yang SY, Bonett RM, Vieites DR, Brandon RA, Wake DB (2005) *Nature* 435:87–90.
11. Smith MA, Green DM (2005) *Ecography* 28:110–128.
12. Lanza B, Vanni S (1981) *Monit Zool Ital* 15:117–122.
13. Delfino M, Razzetti E, Salvidio S (2005) *Atti Mus Civ Stor Nat "G Doria" Genova* 97:45–58.
14. Wilder IW, Dunn ER (1920) *Copeia* 1920:63–68.
15. Wake DB (1966) *Mem So Calif Acad Sci* 4:1–111.
16. Ruben JA, Boicot AJ (1989) *Am Nat* 134:161–169.
17. Wiens JJ, Parra-Olea G, García-París M, Wake D (2007) *Proc R Soc B* 274:919–928.
18. Bromham L, Penny D (2003) *Nat Rev Genet* 4:216–224.
19. Graur D, Martin W (2004) *Trends Genet* 20:80–86.
20. Thorne JL (2003) MULTIDIVTIME v9/25/03 (Department of Genetics and Statistics, North Carolina State University, Raleigh). Available at http://statgen.ncsu.edu/thorne/multidivtime.
21. Müller J, Reisz RR (2005) *BioEssays* 27:1069–1075.
22. Vences M, Vieites DR, Glaw F, Brinkmann H, Kosuch J, Veith M, Meyer A (2003) *Proc R Soc B* 270:2435–2442.
23. San Mauro D, Vences M, Alcobendas M, Zardoya R, Meyer A (2005) *Am Nat* 165:590–599.
24. Zhang P, Chen YQ, Zhou H, Liu YF, Wang XL, Papenfuss TJ, Wake DB, Qu LH (2006) *Proc Natl Acad Sci USA* 103:7360–7365.
25. Kumar S, Hedges SB (1998) *Nature* 392:917–920.
26. Roelants K, Coger DJ, Wilkinson M, Loador SP, Biju SD, Guillaume K, Moriau L, Bossuyt F (2007) *Proc Natl Acad Sci USA* 104:887–892.
27. Marjanovic D, Laurin M (2007) *Syst Biol* 56:369–388.
28. Milner AR (1993) in *The Fossil Record 2*, ed Benton MJ (Chapman & Hall, London), pp 665–679.
29. Gao K, Shubin NS (2003) *Nature* 422:424–429.
30. Zachos J, Pagani M, Sloan L, Thomas E, Billups K (2001) *Science* 292:686–693.
31. Reagan NL, Verrell PA (1991) *Am Nat* 138:1307–1313.
32. Beachy CK, Bruce RC (1992) *Am Nat* 139:839–847.
33. Ruben JA, Reagan NL, Verrell PA, Boucot AJ (1993) *Am Nat* 142:1038–1051.
34. Bruce RC (2005) *Herpetol Rev* 36:107–112.
35. Scotese CR (2001) Earth System History Geographic Information System (PALEOMAP Project, Arlington, Texas), Version 02b.
36. Hendrixson BE, Bond JE (2007) *Mol Phyl Evol* 42:738–755.
37. Kozak KH, Weisrock DW, Larson A (2005) *Proc R Soc B* 273:539–546.
38. Ree RH, Moore BR, Webb CO, Donoghue MJ (2005) *Evolution* 59(11):2299–2311.
39. Donoghue MJ, Smith SA (2004) *Philos Trans R Soc B* 359:1633–1644.
40. Sanmartin I, Enghoff H, Ronquist F (2001) *Biol J Linn Soc* 73:345–390.
41. Lanza B, Pastorelli C, Laghi P, Cimmaruta R (2006) *Atti Mus Civ Stor Nat Trieste* 52:5–135.
42. Storey M, Duncan RA, Swisher CC, III (2007) *Science* 316:587–589.
43. Ericson PGP, Anderson CL, Britton T, Eizanowski A, Johansson US, Källersjo M, Ohlson JI, Parsons TJ, Zuccon D, Mayr G (2006) *Biol Lett* 2:543–547.
44. Bininda-Edmonds ORP, Cardillo M, Jones KE, MacPhee RDE, Beck RMD, Grenyer R, Price SA, Vos RA, Gittleman JL, Purvis A (2007) *Nature* 446:507–512.
45. Wible JR, Rougier GW, Novacek MJ, Asher RJ (2007) *Nature* 447:1003–1006.
46. Moreau CS, Bell CD, Vila R, Archibald SB, Pierce NE (2006) *Science* 312:101–104.
47. Jenkyns HC, Forster A, Schouten S, Sinninghe Damste JS (2004) *Nature* 432:888–892.
48. Gingerich PD (2006) *Trends Ecol Evol* 21:246–253.
49. Smith T, Rose KD, Gingerich PD (2006) *Proc Natl Acad Sci USA* 103:11223–11227.
50. Springer MS, DeBry RW, Douady C, Amrine HM, Madsen O, de Jong WW, Stanhope MJ (2001) *Mol Biol Evol* 18:132–143.
51. Glazko GV, Nei M (2003) *Mol Biol Evol* 20:424–434.
52. Chiari Y, Vences M, Vieites DR, Rabemananjara F, Bora P, Ramilijaona O, Meyer A (2004) *Mol Ecol* 13:3763–3774.
53. Zwickl DJ (2006) PhD dissertation (Univ of Texas, Austin).
54. Ronquist F, Huelsenbeck JP (2003) *Bioinformatics* 19:1572–1574.
55. Swofford DL (2002) *PAUP*: Phylogenetic Analysis Using Parsimony (*and Other Methods)* (Sinauer, Sunderland, MA), Version 4.b10.
56. Shimodaira H, Hasegawa M (1999) *Mol Biol Evol* 16:1114.
57. Wilcox TP, García de Leon FJ, Hendrickson DA, Hillis DM (2004) *Mol Phyl Evol* 31:1101–1113.
58. Hedges SB, Kumar S, Tuinen MV (2006) *BioEssays* 28:770–771.
59. World Conservation Union (IUCN), Conservation International, and NatureServe (2006) Global Amphibian Assessment [World Conservation Union (IUCN), Gland, Switzerland; Conservation International, Arlington, VA; and NatureServe, Arlington, VA], www.globalamphibians.org.
60. Ziegler PA (1988) *Am Assoc Pet Geol Mem* 43:164–196.
61. Veizer J, Ala D, Azmy K, Bruckschen P, Buhl D, Bruhn F, Carden GAF, Diener A, Ebneth S, Godderis Y, *et al.* (1999) *Chem Geol* 161:59–88.
62. Frakes LA, Francis JE, Syktus JL (1992) *Climate Modes of the Phanerozoic* (Cambridge Univ Press, Cambridge, UK).

SI Text Vieites DR, Min M-S, Wake DB 2007 PNAS 104:19903-19907

Phylogenetic Inference. Sequences were translated into amino acids, and aligned by using Clustal X under the default parameters implemented in Bioedit 7.0.5.2 (4); the alignment was adjusted manually, considering amino acid properties. Amino acids missing in >25% of the taxa were excluded from analyses. Phylogenetic analyses were performed in two ways. First, we concatenated the data from the three genes into a single dataset and performed maximum likelihood (ML) and Bayesian inference (BI), and second, we repeated the analyses with each nuclear marker independently to test for congruency in the phylogenetic signal. For BI analyses, we partitioned our dataset by gene and codon position, and determined the evolutionary model and parameters that best fit each partition (SI Table 2) using the Akaike Information Criterion implemented in MrModeltest version 2.2 (5). To avoid overpartitioning our dataset, partitions with similar parameters were combined. BI was performed with Mr Bayes v3.1 (6). We ran two independent analyses consisting of four Markov chains sampled every 1,000 generations for 40 million generations, with a ML starting tree, default priors, and the option prset ratepr set as variable. We used the online program AWTY (7) to check for stationarity and estimate the burnin parameter. After discarding the first 20 million generations, remaining trees from both analyses were combined, and a 50% majority rule consensus tree was calculated by using PAUP* 4b10 (8). Nonparametric bootstrap ML analyses were conducted using Garli v0.94 (9). We chose this program because, unlike other newly developed programs for ML inference, Garli provides likelihood estimations directly comparable to those obtained with PAUP*, but it performs the calculations much faster. One thousand bootstrap repetitions were run for the concatenated dataset, and 100 were run for each nuclear marker. Analyses were repeated three times to check for congruence. Best fitting evolutionary models and parameters were determined by using Modeltest 3.6 (10). Alternative topologies were tested with SHT (11) as implemented in PAUP* 4b10 (8), by using 2,000 bootstrap replicates and full optimization settings.

Divergence Dating and Evolutionary Rates. We tested for constancy of evolutionary rates by performing Bayesian relative rate tests (BRRT) (13).

Cadence v1.08 (12) calculated the posterior probability distribution of the summed branch lengths from the most recent common ancestor (MRCA) of the ingroup to each terminal taxon, using the last 20,000 trees remaining after burnin from one of the BI runs for the whole partitioned dataset. Median and confidence interval were calculated for each taxon. The confidence interval is that within which 95% of the observed distances to the MRCA in all trees fall (12). Due to the observed slower rates of evolution within salamanders compared with other clades, the analysis was performed both for the whole dataset and for a subset of taxa including all taxa in subfamily Plethodontinae (Fig. 1) using spelerpines as outgroups. We used BRRT to determine whether evolutionary rates varied among plethodontid taxa and if so, whether they are associated with any major cladogenetic or biogeographic events. We considered that two taxa have significantly different rates of evolution when their 95% confident intervals do not overlap.

To estimate the divergence times among clades, we used a multiple calibration Bayesian approach implemented in the package MULTIDIVTIME (13, 14). This method applies a relaxed molecular clock, not requiring the assumption of constant evolutionary rates among genes and lineages, allowing the use of prior constraints on divergence times. For this reason, it was chosen instead of penalized likelihood (15), because it estimates the age of the root from a prior instead of fixing it at a particular time. To test the potential influence of priors, fossil age constraints, and our partitioning strategy on time estimates, we performed several analyses trying different combinations of these parameters. The dataset was divided into the same partitions as in the BI for the phylogeny, and model parameters were estimated both for each partition and for the whole concatenated dataset without partitioning, by using baseml (PAML v3.15; ref. 16) and selecting the F84+gamma model. ML estimates of branch lengths with their variance–covariance matrices were calculated with Estbranches (Multidistribute package v 9/25/03; ref. 14) and used as input for MULTIDIVTIME. The prior for the mean of the ingroup root age (rttm) was set to 3.44 time units, where 1 time unit represents 100 mya, corresponding to the split between amphibians and amniotes. The standard deviation of the prior distribution (rttmsd) was set to the mean of rttm (its maximum value), to avoid violation of the

definition of a prior (17). We also tested the effect on time estimates of constraining rttmsd to 0.2 (20 mya), as was suggested for that split (18). The mean and standard deviation for rate at root node in this dataset were set to 0.076 (substitutions per site per 100 mya), empirically calculated as the median of the substitution path lengths between each tip and the root in this dataset, divided by rttm (14). Mean and standard deviation of prior for Brownian motion constant were set to 0.43. We also tested the potential effect of the "bigtime" parameter by using 5 and 4.2 time units, corresponding to 500 mya, and the maximum time for the 419–408 mya lungfish–tetrapod split (2), respectively. Analyses were run for 3 ´ 106 generations after a burnin of 105 generations, with the MCMC chain sampled every 100 cycles. A second independent run for 106 generations was performed to test for convergence.

The number of age constraints and their reliability can affect divergence time estimates (19). Because the salamander fossil record is uneven, we included several well constrained splits outside amphibians for our divergence time estimation, and used nine calibration events based on amphibian fossils. Two major events in tetrapod evolution that are well characterized in the fossil record have been suggested by paleontologists to be suitable for molecular clock calibrations, the split between birds and crocodiles (251–243 mya) and the split between birds and squamates (257–252 mya) (2). However, the maximum age estimates for these two constraints have recently been criticized (3). Because of this controversy over the value of constraining those nodes of the tetrapod fossil record, we performed analyses with and without those constraints to test their potential effects on the divergence time estimation. We also included in those tests the widely used date for the split between Theropsida and Sauropsida (332–360 mya). For the other constraints less well defined from the paleontological perspective, we used minimum ages to avoid overconstraining our estimates: Anura and Caudata split at 230 mya (fossil record of frog ancestor Triadobatrachus massinoti, Triassic; ref. 20); split of Hynobiidae and Cryptobranchidae at 155 mya (Chunerpeton tianyiensis, Late Jurassic; ref. 21); split of pipid frogs from their sister group at 140 mya (records of Mesozoic fossil pipids; ref. 22); split between Amphiumidae and Plethodontidae at 65.5 mya (Proamphiuma cretacea, Late Cretaceous; ref. 23); split of Ambystoma and Dicamptodon split at 55.8 mya (Dicamptodon antiquus, Late Paleocene; ref. 24); split between Pleurodeles and

Tylototriton at 44 mya (Chelotriton weigelti; ref. 25); a minimum age of Hydromantes in Europe at 13.65 mya (Hydromantes sp., Middle Miocene; ref. 26).

We compared the effect of different priors, partitions and number of fossil constraints on the time estimates for major cladogenic events. Comparisons included all possible combinations of parameters rttmsd set to 175 mya or 20 mya, bigtime set to 420 mya (split between tetrapods and lungfishes) or 500 mya, for both the partitioned dataset and the unpartitioned dataset. Those analyses were done including all our fossil constraints, but we also performed two analyses with rttmsd set to 175 and 20 mya, respectively, including only two constraints, which were suggested as the most suitable for divergence dating from the paleontological perspective (2). Among the priors, bigtime seems to have an effect on the estimates of ancient nodes, with no major effects on nodes younger than 130 mya for this dataset, but a tendency to make the nodes of basal splits older than in other estimates. The worst combination of parameters seems to be bigtime set to 500 mya and rttmsd set to 20 mya, resulting in younger estimates for all nodes. We tested the performance of these estimations with nodes with known fossil records. One good example of this underestimation is the case of European Hydromantes. The oldest fossil available is dated at 13.65 mya (26). The estimates given by all combinations but bigtime 500 / rrtmsd 20 gave very similar estimates with a confidence interval between 13.8 and 26–27 mya, compatible with the fossil data available. However, the bigtime 500 / rttmsd 20 combination gave a 95% confidence interval between 1.7 and 11.4 mya, younger and in conflict with the fossil and geologic evidence. When bigtime was set to 400 mya, there was no effect of rttmsd on the estimates. The unpartitioned dataset gave similar results to the partitioned one when rttmsd was set to 175 mya, with a tendency to estimate the younger nodes as older. The estimates calculated by using only the two well constrained bird–lizard and bird–crocodile splits gave results that overlapped with the confidence intervals calculated with other approaches. Times estimated for splits older than 160 mya were very close to those calculated with the whole fossil dataset; however, estimated young splits were in conflict with the fossils.

Phylogenetically Derived Biogeographic Reconstructions. Posteriori optimization of the geographic distributions of terminal taxa was

done following Beard (27). Our tree topology reconstructs North America as the continent on which the Plethodontid family and basal clades arose. The Eurasian plethodontids are deeply nested within the North American clades. Although the origin of those clades in North America and their divergence times seem clear, the ancestral distribution ranges, routes, and directions for dispersal need further testing. To test the likelihood of different ancestral range scenarios and directions of dispersal, ML inference of the evolution of geographic ranges was explored with Lagrange 1.0 (28). This method was preferred instead of a dispersal–vicariance analysis, as implemented in DIVA, because it takes into account more parameters including branch lengths. It uses a phylogenetic hypothesis with divergence time estimates, together with dispersal capacities and extinction rates, allowing the implementation of a paleogeographic model, which permits specification of probabilities of dispersal, or the lack thereof, between regions in geologic time. The method provides likelihood values for the different biogeographic scenarios, accounting for both the phylogenetic hypothesis and the paleogeographic model. Scripts were programmed in PERL language and run in Python 2.5. We divided the Holarctic in four areas: western North America (WNA), eastern North America (ENA), eastern Eurasia (EE), and western Eurasia (WE). Paleogeographic connections between these landmasses were gathered form the literature. An epicontinental seaway divided WNA and ENA during the Cretaceous (110–70 Mya), extending in some areas into the Paleocene although connections were already available (29). The Turgai sea divided EE and WE at least from the late Jurassic to the Oligocene, although connections were suggested for plants during the last 50 Mya. Therefore we set up the probability of dispersal success to one over this time period (28, 30). The Beringian land bridge was opening and closing periodically during the Mesozoic and Cenozoic, breaking up finally in the Pliocene (»5 Mya) (30). The connection between eastern North America and western Eurasia was possible through Greenland and Ellesmere Island, with two independent connections that opened at different periods of time: ENA to Greenland via Ellesmere Island, and Greenland to WE. The North Atlantic land connection between Greenland and WE broke in the early Eocene (»55 Mya; ref. 31), and paleogeographic reconstructions suggest that the land connection between Northern Greenland and Ellesmere Island and ENA re-opened again from the early Paleozoic (» 65 Mya; ref. 32). Following Ree et al. (28), we performed several analyses with low and high

rate scenarios of dispersal and extinction. Parameter values for lineage dispersal (lD) and extinction (lE) included "high" and "low" rates. Data on dispersal capacities for plethodontids were gathered from Smith and Green (33). The mean, minimum, and maximum reported dispersal capacities were used in the analyses, ranging from lD = 0.05 to 0.09, although slowest rates were explored ranging from lD = 0.005 to 0.009 (28). Extinction rates of amphibians are not well known, hence we used three rates of lE 0.001, 0.01 and a high rate of 0.2926 corresponding to the average under a constant diversification model for amphibians (18). For each internode and pair of parameter values, 105 simulations were run for each range in Lagrange to estimate the range transition matrices. The highest overall likelihood was obtained at a low rate of dispersal and extinction, where lD = 0.005 and lE = 0.001. Statistical significance of likelihood differences between biogeographic scenarios was assessed by using a conventional cutoff value of two log-likelihood units (28, 34).

Taxonomy. For effective communication, we use our new higher taxonomy throughout. This taxonomy is based on principles of phylogenetic systematics from our analysis (Fig. 1). Unless otherwise specified, italicized words refer to genera. Taxonomy of Hydromantes (sensu lato) is contentious (35, 36). Our phylogenetic analysis supports the existence of three clades within Hydromantes, with substantial divergences among them. To stabilize taxonomy, we raise these subgenera to generic rank as Hydromantes Gistel 1848 for the North American species (H. shastae, H. platycephalus, and H. brunus), Atylodes Gistel 1868 for the southwestern Sardinian species (A. genei), and Speleomantes Dubois 1984 for the remaining European species (S. italicus, S supramontis, S. imperialis, S. flavus, S. ambrosii, and S. strinatii). The new taxonomy is as follows:

Family Plethodontidae

Subfamily Plethodontinae

Genus (G) Aneides

Supergenus (Sg) Desmognathus (Desmognathus, Phaeognathus)

G Ensatina

Sg Hydromantes (Atylodes, Hydromantes, Speleomantes)

G Karsenia

G Plethodon

Subfamily Hemidactyliinae

G Hemidactylium

G Batrachoseps

Sg Bolitoglossa (Bolitoglossa, Bradytriton, Chiropterotriton,

Cryptotriton, Dendrotriton, Ixalotriton, Lineatriton, Nototriton,

Oedipina, Parvimolge, Pseudoeurycea, Thorius)

Tribe Spelerpini (Eurycea, Gyrinophilus, Pseudotriton, Stereochilus).

1. Müller J, Reisz RR (2005) BioEssays 27:1069–1075.

2. Hedges SB, Kumar S, Tuinen MV (2006) BioEssays 28:770–771.

3. Poux C, Madsen O, Marquard E, Vieites DR, Jong WW, Vences M (2005) Syst Biol 54:719–730.

4. Hall TA (1999) Nucleic Acids Symp Ser 41:95–98.

5. Nylander JAA (2004) MrModeltest v2.2 (program distributed by the author, Evolutionary Biology Centre, Uppsala University, Uppsala).

6. Ronquist F, Huelsenbeck JP (2003) Bioinformatics 19:1572–1574.

7. Wilgenbusch JC, Warren DL, Swofford DL (2004) AWTY: A system for graphical exploration of MCMC convergence in Bayesian phylogenetic inference http://king2.csit.fsu.edu/CEBProjects/awty/awty_start.php

8. Swofford DL (2002) PAUP*: Phylogenetic analysis using parsimony (*and other methods) (Sinauer Associates, Sunderland, MA), Version 4.b10.

9. Zwickl DJ (2006) Ph.D. dissertation (Univ of Texas, Austin).

10. Posada D, Crandall KA (1998) Bioinformatics 14:817–818.

11. Shimodaira H, Hasegawa M (1999) Mol Biol Evol 16:1114.

12. Wilcox TP, García de Leon FJ, Hendrickson DA, Hillis DM (2004) Mol Phyl Evol 31:1101–1113.

13. Thorne JL, Kishino H (2002) Syst Biol 51:689–702.

14. Thorne JL (2003) MULTIDIVTIME v9/25/03 (Department of Genetics and Statistics, North Carolina State University). Available at http://statgen.ncsu.edu/thorne/multidivtime.

15. Sanderson MJ (2002) Mol Biol Evol 19:101–109.

16. Yang Z (1997) CABIOS 15:555–556.

17. San Mauro D, Vences M, Alcobendas M, Zardoya R, Meyer A (2005) Am Nat 165:590–599.

18. Roelants K, Coger DJ, Wilkinson M, Loador SP, Biju SD, Guillaume K, Moriau L, Bossuyt F (2007) Proc Natl Acad Sci USA 104:887–892.

19. Graur D, Martin W (2004) Trends Genet 20:80–86.

20. Rage JC, Rocek Z (1989) Palaeontographica Abt A 206:1–16.

21. Gao K, Shubin NS (2003) Nature 422:424–429.

22. Rocek Z (2000) in Amphibian Biology, eds Heatwole H, Carroll RL (Surrey Beatty, Chipping Norton, Australia), pp 1295–1331.

23. Gardner JD (2003) J Vert Paleontology 23:769–782.

24. Taylor BG, Fox RC (1993) Can J Earth Sci 30:814–818.

25. Milner AR (2000) in Amphibian Biology, eds Heatwole H, Carroll RL (Surrey Beatty, Chipping Norton, Australia), pp 1412–1444.

26. Venczel M, Sanchiz B (2005) Amphibia–Reptilia 26:408–411.

27. Beard KC (1998) Bull Carnegie Mus Nat Hist 34:5–39.

28. Ree RH, Moore BR, Webb CO, Donoghue MJ (2005) Evolution 59(11):2299–2311.

29. Steven SM (1999) Earth System History (Freeman, New York), pp 487–489.

30. Tiffney BH, Manchester SR (2001) Int J Plant Sci 162:S3–S17.

31. Storey M, Duncan RA, Swisher III, CC (2007) Science 316:587–589.

32. Ziegler PA (1988) Am Assoc Petroleum Geol Memoir 43:164–196.

33. Smith MA, Green DM (2005) Ecography 28:110–128.

34. Edwards AWF (1992) Likelihood (Johns Hopkins Univ Press, Baltimore).

35. Wake DB, Salvador A, Alonso-Zarazaga MA (2005) Amphibia–Reptilia 26:543–548.

36. Crochet PA (2007) Amphibia–Reptilia 28:170–172.

Table 1. Results of non-parametric likelihood ratio tests (SHT), showing the topologies tested, their likelihood scores, and the significance of the difference in likelihood score as compared to the best tree. Significances of $P<0.05$ are marked with an asterisk.

	Description of tree permutation	Likelihood (-lnL)	*P* value
1	best ML tree	25447.86913	----
2	*Karsenia* sister to *Aneides*	25455.66648	0.7035
3	*Karsenia* sister to (*Phaeognathus*+*Desmognathus*)	25455.77661	0.6990
4	*Karsenia* sister to (*Ensatina* ((*Phaeogathus*+*Desmognathus*)+ *Aneides*))	25454.80029	0.8435
5	*Karsenia* sister to *Ensatina*	25464.95178	0.4905
6	*Karsenia* sister to *Plethodon*	25468.46811	0.4000
7	*Karsenia* sister to clade B (see results)	25465.61581	0.4905
8	(*Atylodes*+*Speleomantes*) sister to (*Karsenia*+*Hydromantes*)	25525.00450	0.0025*
9	*Hydromantes* sister to (*Karsenia*(*Atylodes*+*Speleomantes*))	25525.00450	0.0025*
10	*Atylodes* sister to (*Hydromantes* + *Speleomantes*)	25517.15431	0.0065*
11	Eastern *Plethodon* sister to (Western *Plethodon*+ *Aneides*)	25555.51378	0.0000*

Table 2. Comparison of divergence time estimates calculated in MULTIDIVTIME (see methods). Values represent mya, and minimum and maximum values correspond to the 95% confidence interval of time estimation. Two of the several combinations tested in the analyses are shown, one with maximum divergence times constrained in the nodes Aves - Squamata and Aves - Alligatoridae, and the other without these constraints using only the minimum age proposed by Müller & Reisz[1]. Hedges *et al.*[2], in response to Müller & Reisz[1], proposed not to use maximum divergences on these nodes because they could underestimate divergence times in the whole tree. However, our analyses suggest that whether or not one constrains those nodes has no effect on the estimated ages in the rest of the tree. Nevertheless, without the maximum constraints, the ages of the bird - crocodilian split under the two estimates overlap, while the bird - squamate split without the maximum divergence is ca. 30 mya older. This suggests that the most conservative scenario is to follow Hedges *et al.* [2] in this case, not constraining this node, which should be tested in the future with a robust and comprehensive tetrapod phylogeny.

	With maximum fossil constraints				Without maximum fossil constraints			
Taxonomic content	Mean	SD	Min	Max	Mean	SD	Min	Max
H.brunus - H.platicephalus	4	3	0	11	4	3	0	11
H.shastae - (H.brunus+ H.platicephalus)	8	4	2	16	8	4	2	17
Atylodes - Speleomantes	16	3	14	24	17	3	14	24
Small - Big Eastern *Plethodon*	17	5	8	29	18	6	8	30
Central - Western *Aneides*	26	6	15	39	26	7	15	41
Stereochilus - Pseudotriton	31	7	18	47	32	8	19	49
Eastern- Central *Aneides*	35	7	22	50	36	8	22	52
Eastern - Western *Plethodon*	39	8	25	56	40	8	26	59
Gyrinophilus - (Pseudotriton + Stereochilus)	40	8	27	57	42	8	27	60
Hydromantes - (Speleomantes + Atylodes)	41	7	28	57	41	8	28	58
Desmognathus - Phaeognathus	46	8	31	62	47	8	32	65
Eurycea - Gyrinophilus	48	9	33	66	50	9	34	69
Pleurodeles - Tylototriton	49	4	44	60	49	5	44	61
Aneides - (Desmognathus - Phaeognathus)	51	8	36	68	52	9	37	71

Ensatina - *(Aneides, Phaeognathus* + *Desmognathus)*	61	9	45	80	63	9	46	83
Plethodon - *Ensatina*	67	9	50	86	69	10	51	89
Karsenia – *Sg.* Hydromantes	67	9	50	87	69	10	51	90
Bolitoglossa - *Batrachoseps*	73	11	53	96	75	11	55	99
(Karsenia + *Hydromantes)* - other Plethodontinae	74	10	57	95	77	10	58	98
Hemidactylium - *(Batrachoseps* + *Bolitoglossa)*	84	11	64	107	87	11	67	110
Spelerpinae - (Bolitoglossinae + *Hemidactylium*)	88	11	68	111	91	11	70	114
Plethodontinae – Hemidactylinii	94	11	74	117	96	11	76	120
Dicamptodon - *Ambystoma*	134	15	106	164	137	15	109	168
Amphiuma - Plethodontidae	146	14	120	176	150	15	122	180
Hynobiidae - *Cryptobranchidae*	167	10	155	192	169	11	156	195
Rhyacotritonidae - (Amphiumidae + Plethodontidae)	168	14	141	197	172	14	145	201
Pipidae - Ascaphidae	179	19	146	218	181	19	146	220
Salamandridae - (Ambystomatidae + Dicamptodontidae)	188	15	160	218	192	15	163	222
(Hynobiidae + *Cryptobranchidae)* - other salamanders	227	13	203	254	230	13	206	258
Aves - Alligatoridae	246	2	243	250	251	7	243	268
Aves - Squamata	255	1	252	257	283	12	261	307
Anura - Caudata	322	14	293	349	324	14	295	350
Theropsida - Sauropsida	328	9	312	344	333	8	315	344
Amniota - Amphibia	350	6	336	359	351	6	337	360

Table 3. Voucher specimens, Museum of Vertebrate Zoology number (MVZ), and Genbank accession numbers.

Museum number	*Taxa*	POMC	BDNF	RAG
---	*Alligator mississipiensis*	EU275842	EU275888	AF143724
132964	*Ambystoma rosaceum*	EU275841	EU275887	AY583345
241480	*Amphiuma tridactylum*	EU275817	EU275863	AY650128
204245	*Andrias davidianus*	EU275843	EU275889	AY650142
158353	*Aneides aeneus*	EU275844	EU275890	AY691701
219942	*Aneides ferreus*	EU275845	EU275891	EU275805
170983	*Aneides flavipunctatus*	EU275848	EU275894	EU275808
219973	*Aneides flavipunctatus*	EU275849	EU275895	EU275809
226110	*Aneides hardii*	EU275811	EU275857	EU275780
249828	*Aneides lugubris*	EU275847	EU275893	EU275807
220991	*Aneides vagrans*	EU275846	EU275892	EU275806
187732	*Ascaphus truei*	EU275850	EU275896	AY323754
---	*Atylodes genei*	EU275840	EU275886	EU275804
156447	*Batrachoseps major*	EU275855	EU275901	AY650126
225875	*Bolitoglossa sp. nov.*	EU275851	EU275897	EU275810
145017	*Desmognathus brimleyorum*	EU275819	EU275865	EU275786
224931	*Desmognathus fuscus*	EU275812	EU275858	EU275781
192601	*Dicamptodon tenebrosus*	EU275824	EU275870	EU275789
236171	*Ensatina eschscholtzii*	EU275816	EU275862	EU275785
225074	*Eurycea bislineata*	EU275815	EU275861	EU275784
---	*Gallus gallus*	71895056	DQ124361	AF143730
173504	*Gyrinophilus porphyriticus*	EU275853	EU275899	AY583349
225078	*Hemidactylium scutatum*	EU275852	EU275898	AY691711
---	*Homo sapiens*	BT019918	X60201	NM000448
238576	*Hydromantes brunus*	EU275825	EU275871	EU275790
240733	*Hydromantes platicephalus*	EU275828	EU275874	EU275793
230651	*Hydromantes shastae*	EU275829	EU275875	EU275794
197240	*Hynobius sonani*	EU275818	EU275864	AY650144
246033	*Karsenia koreana*	EU275822	EU275868	AY887135
173507	*Phaeognathus hubrichti*	EU275814	EU275860	EU275783
220003	*Plethodon elongatus*	EU275836	EU275882	AY650120
215255	*Plethodon fourchensis*	EU275838	EU275884	EU275802
137290	*Plethodon hoffmani*	EU275837	EU275883	EU275801
206567	*Plethodon jordani*	EU275835	EU275881	EU275800
---	*Plethodon larselli*	EU275839	EU275885	EU275803
145037	*Plethodon ouachitae*	EU275831	EU275877	EU275796
215256	*Plethodon serratus*	EU275830	EU275876	EU275795
206570	*Plethodon teyahalee*	EU275834	EU275880	EU275799
236241	*Plethodon vandykei*	EU275833	EU275879	EU275798
225739	*Plethodon yonahlossee*	EU275832	EU275878	EU275797
235673	*Pleurodeles poireti*	EU275820	EU275866	EU275787
---	*Protopterus sp.*	4760914	EU275856	AY442928
137304	*Pseudotriton ruber*	EU275854	EU275900	AY650123
222581	*Rhyacotriton variegatus*	EU275823	EU275869	AY691693
163996	*Speleomantes italicus*	EU275826	EU275872	EU275791
163997	*Speleomantes italicus*	EU275827	EU275873	EU275792
---	Squamata	AB128826	DQ385335	AY662590
233227	*Stereochilus marginatus*	EU275813	EU275859	EU275782
236638	*Tylototriton wenxianensis*	EU275821	EU275867	EU275788
---	*Xenopus laevis*	X05940	EF035623	L19324

Table 4. Best-fitting models of evolution and parameters selected for each codon position with hierarchical likelihood methods. Codon positions with similar model and model parameters were regrouped into the same partition[3]. Symbols and abbreviations represent: *Π*, frequency of base; *Tratio*, transition / transversion ratio; *rmat*, rate matrix; *PInvar*, proportion of invariable sites; *alpha*, shape of gamma distribution.

Gene	Codon position	Length	πA	πC	πG	Best model	Tratio or Rmat	alpha	Pinvar	Partition number
POMC	1	160	0.30	0.23	0.34	TVM+G	(2.9 2.1 0.9 0.8 2.1)	0.64	0	1
	2	160	0.40	0.17	0.27	GTR+G	(2.4 2.9 1.6 3.5 6.9)	0.50	0	2
	3	160	0.30	0.22	0.34	TVM+G	(3.4 2.4 1.1 0.9 2.4)	0.63	0	1
BDNF	1	235	0.29	0.20	0.31	GTR+G	(4.7 3.2 1.9 0.9 13.8)	0.32	0	3
	2	236	0.25	0.25	0.25	TrNef+I	(1.0 4.2 1.0 1.0 1.3)	0.02	0.75	4
	3	236	0.25	0.25	0.25	SYM+G	2.95	0,93	0	5
RAG1	1	485	0.32	0.21	0.27	GTR+I+G	(2.3 1.8 0.9 0.8 3.8)	0.94	0.39	6
	2	485	0.35	0.20	0.16	GTR+I+G	(2.1 8.9 1.5 5.6 3.5)	0.64	0.57	7
	3	486	0.27	0.24	0.22	TrN+I+G	(1.0 4.8 1.0 1.0 5.6)	3.72	0.02	8

Primers developed for this study: BDNF_DRV_F1: 5'-ACCATCCTTTTCCTKACTATGG-3'; BDNF_DRV_R1: 5'-CTATCTTCCCCTTTTAATGGTC-3'; POMC_DRV_F1: 5'-ATATGTCATGASCCAYTTYCGCTGGAA-3'; POMC_DRV_R1: 5'-GGCRTTYTTGAAWAGAGTCATTAGWGG-3'; RAG_DRV_PIF: 5'-ACAACTGGACGRCAGATTTTCCAGCC-3'; RAG_DRV_PIR: 5'-GTGATGCTTCAGCACATCCTC-3'.